

See discussions, stats, and author profiles for this publication at: <https://www.researchgate.net/publication/220043573>

# Solvation Sheath of Li<sup>+</sup> in Nonaqueous Electrolytes and Its Implication of Graphite/Electrolyte Interface Chemistry

ARTICLE *in* THE JOURNAL OF PHYSICAL CHEMISTRY C · MAY 2007

Impact Factor: 4.77 · DOI: 10.1021/jp068691u

CITATIONS

61

READS

79

## 5 AUTHORS, INCLUDING:



**Kang Xu**

Army Research Laboratory

175 PUBLICATIONS 5,617 CITATIONS

SEE PROFILE



**Yiufai Lam**

University of Maryland, College Park

2 PUBLICATIONS 84 CITATIONS

SEE PROFILE



**Shengshui Zhang**

Army Research Laboratory

169 PUBLICATIONS 5,746 CITATIONS

SEE PROFILE



**Richard Jow**

Army Research Laboratory

170 PUBLICATIONS 4,826 CITATIONS

SEE PROFILE

# Solvation Sheath of Li<sup>+</sup> in Nonaqueous Electrolytes and Its Implication of Graphite/Electrolyte Interface Chemistry

Kang Xu,<sup>\*,†</sup> Yiufai Lam,<sup>‡</sup> Sheng S. Zhang,<sup>†</sup> T. Richard Jow,<sup>†</sup> and Timothy B. Curtis<sup>†,§</sup>

Electrochemistry Branch, Sensor and Electron Devices Directorate, U.S. Army Research Laboratory, Adelphi, Maryland 20783, and Department of Chemistry and Biochemistry, University of Maryland, College Park, Maryland 20783

Received: December 18, 2006; In Final Form: March 5, 2007

The formation chemistry of graphite/electrolyte interface and its dependence on electrolyte bulk composition were investigated by conducting electrochemical impedance analyses on interfaces systematically formed in various electrolytes and NMR identification of surface species harvested therefrom. The interpretation of these analyses strongly suggests that Li<sup>+</sup> solvation sheath structure is central in defining the anode surface chemistry, because solvent molecules preferentially recruited by Li<sup>+</sup> into the solvation sheath would be preferentially reduced on graphene surface upon initial charge of the electrode. Due to the preference of Li<sup>+</sup> in binding the more polar molecules from the electrolyte solvent mixture, the contributions from cyclic and linear carbonates to the interface chemistry are unsymmetrical, and ethylene carbonate, the universal cosolvent in all electrolyte formulations, consequently becomes the favored chemical source for the interfacial ingredients. Since the chemical composition of the interface dictates Li<sup>+</sup> transport kinetics at low temperatures, the understandings about how the electrolyte cosolvents share the responsibility for the graphite/electrolyte interfacial chemistry will benefit the efforts to tailor an interface that is more tolerant toward the operation of Li ion devices at sub-zero temperatures.

## Introduction

Electrochemistry is the science of chemistry and processes at the interfaces between electrolytes and electrodes, and no rechargeable battery chemistry serves as a better example than that of Li ion in demonstrating what a critical role those interfaces could play in ensuring successful operation of a device. Almost immediately upon the birth of this youngest battery chemistry, it was recognized that the selection of electrolyte components, especially solvents, dictates whether the graphitic anodes could stably support the reversible Li<sup>+</sup> intercalation and de-intercalation at low potentials and provide the device with maximal energy density.<sup>1</sup> The polar and aprotic molecules, mainly from the family of dialkyl- and cyclic alkene esters of carbonic acid, thus became the prevailing electrolyte solvents, and their surface reductions on graphitic carbonaceous electrodes form the essential key to understand the disciplines of Li ion chemistry. The ensuing graphite/electrolyte interface is believed to consist of the decomposition products from these carbonates upon the initial charge of the Li ion cell, and its nomenclature “solid electrolyte interphase” (SEI), though transplanted from an earlier concept developed for the passivation chemistry of metallic lithium in nonaqueous solutions,<sup>2</sup> suggests its selectivity toward the migrations of electrolyte components, i.e., allowing Li<sup>+</sup> to diffuse through while filtering away solvent molecules and insulating the electron tunneling between graphene interior and the bulk electrolyte (Figure 1a). The former ensures the reversible Li<sup>+</sup> intercalation into or de-intercalation from the graphene structure as anode potential

cycles, and the latter prevents sustained surface-reductions of solvents and maintains the physical integrity of the electrode.

The knowledge about the chemical nature of SEI mainly came from the surface characterization studies by Aurbach et al., who unequivocally established that lithium ethylene dicarbonate (LEDC), produced via the single electron reduction of the cyclic solvent ethylene carbonate (EC), is responsible for the above-mentioned protective functions of the interfacial layer (Scheme 1a).<sup>3</sup>

This single-electron reduction path was extended to linear carbonates (Scheme 1b) when Ein-Eli discovered that electrolytes based on neat linear carbonates could also support the reversible Li ion chemistry with graphitic anode.<sup>4</sup> However, it was never clear how cyclic and linear carbonates share the responsibility of contributing to SEI chemistry in electrolytes that are based on mixed solvents. Apparently, any knowledge about this source distribution of SEI ingredients would be highly desirable and of significance, because it is such mixtures of cyclic and linear carbonates, either in binary or higher order compositions, that constitute the skeletal formulations of the electrolytes overwhelmingly used in commercial Li ion devices, despite the minute variations among manufacturers.

More recent studies on the graphite/electrolyte interface employing in situ Fourier-transformed infrared (FTIR) spectroscopy revealed a more complicated picture of the chemical species on the electrodes harvested from actual Li ion devices.<sup>5</sup> While lithium salts of oxalate and dicarbonates with longer alkene chains were also proposed as reduction products of dialkyl or alkene carbonates—therefore, the possible ingredients of the interface—the participation of linear carbonates in the formation chemistry of SEI was especially placed under question, as spectroscopic evidence supporting Scheme 1b was almost always elusive.<sup>6,7</sup> It seems that cyclic carbonate (EC)

\* Corresponding author. E-mail: cxu@arl.army.mil.

† U.S. Army Research Laboratory.

‡ University of Maryland.

§ Summer student from Norwich University, Northfield, VT 05663-1097.

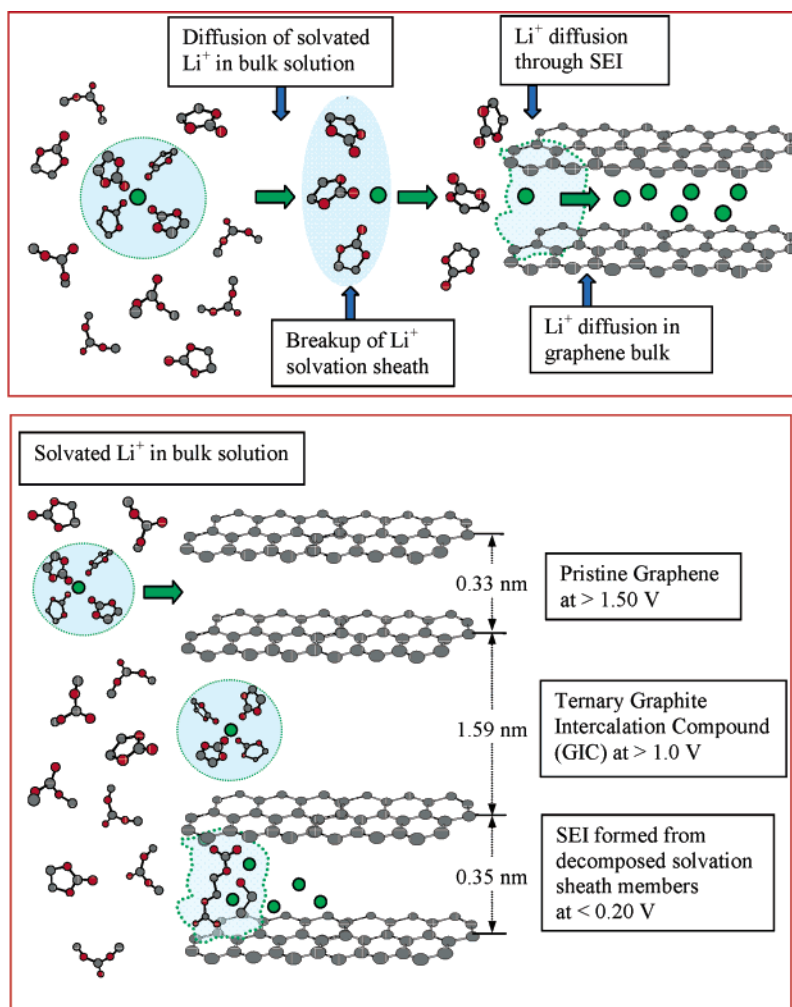
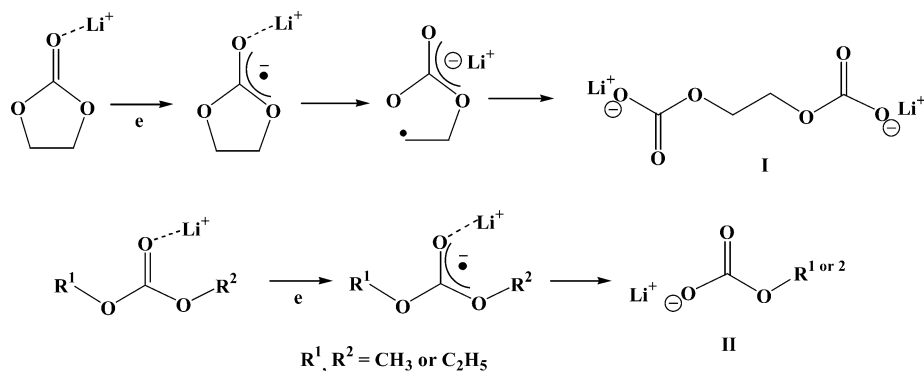


**Figure 1.** Schematic descriptions of (a, upper) the post-SEI journey of a solvated  $\text{Li}^+$  from solution bulk to graphene interior, where desolvation is the rate-determining step (ref 12), and (b, below) the dependence of surface chemistry on  $\text{Li}^+$  solvation sheath, whose members serve as chemical sources of SEI upon the initial charge of graphitic anode. The interlayer distances were based on the X-ray diffraction data of a ternary GIC formed in PC-electrolyte by Besenhard and Winter et al. (ref 22), and the tetrahedron structure of  $\text{Li}^+$  solvation sheath was generated by CS ChemBats3D of CambridgeSoft Corp. with MM2 energy minimization.

#### SCHEME 1: Electrochemical Reductions of (a) EC and (b) Linear Carbonates through Single-Electron Path



possesses an unsymmetrical precedence in participating surface reductions, despite its relatively low population in most electrolyte formulations.<sup>6</sup>

In an effort to understand the limiting factors that control the low-temperature transport mechanisms in Li ion devices, we recently studied the electrochemical impedance spectrum (EIS) of graphitic anodes at the characteristic lithiation potential of 0.15 V in a wide temperature range.<sup>8</sup> When examining the temperature dependences of impedance spectra in the context of varying electrolyte composition, we unexpectedly encountered

the fundamental issue concerning the distribution of the SEI-ingredient sources. Through a rather characteristic correlation between the “charge-transfer” activation energies and the bulk electrolyte compositions, it was found that the  $\text{Li}^+$  solvation sheath structure seems to vary in a way that is dictated by the tendency of  $\text{Li}^+$  to preferentially bind cyclic rather than linear carbonates. A series of new questions were thus raised: does this preference of  $\text{Li}^+$  for solvation sheath members translate into any asymmetry when SEI ingredient are formed from the reductive decompositions of the electrolyte components during

the initial charge, consequently resulting in an interface that is primarily originated from one particular cosolvent? How will the bulk electrolyte composition affect this asymmetry? And how is the kinetics of Li ion device at sub-zero temperatures coupled with the surface chemistry thus formed? In the present work, we try to address these questions by combining the phenomenological tool of EIS with the direct chemical analyses on the surface species as harvested from the cycled graphitic anodes. The fundamental understanding of SEI formation chemistry would undoubtedly assist us in the efforts to tailor a desired electrode/electrolyte interface, which by far remains the least understood yet most determining subcomponent in Li ion devices.

## Experimental

Lithium hexafluorophosphate (LiPF<sub>6</sub>) and lithium tetrafluoroborate (LiBF<sub>4</sub>) were from Stellar Chemifa Inc. and used as received. Ethylene carbonate (EC), ethylmethyl carbonate (EMC), and dimethyl carbonate (DMC) were from Ferro Corp. and redistilled after storing over 3A molecular sieves. The electrolyte solutions were made in a glovebox with moisture level below 5 ppm, and cells were assembled in a dryroom where dew point is below −80 °C.

In electrochemical impedance spectrum (EIS) studies, a three electrode test cell as previously described was used, in which a composite MCMB (85% active agents, 5% carbon black and 10% PVDF) coated on Cu foil of 20.27 cm<sup>2</sup> served as working and two Li discs of 31.67 cm<sup>2</sup> and 2.0 cm<sup>2</sup> as counter and reference electrodes, respectively.<sup>8</sup> Before each impedance measurement on a Solartron SI 1260 Impedance/Gain-Phase Analyzer, the cells were formed at the rate of C/10 for 5 cycles and then stabilized at 0.1500 ± 0.0001 V by a Solartron SI 1287 Electrochemical Interface till residual current densities dropped below C/200 (~200 μA). AC impedance measurements were carried out in the frequency range of 0.01–10<sup>6</sup> Hz with an AC perturbation of 10 mV in amplitude, while a DC bias equivalent to the cell potential (0.1500 V vs Li reference) was applied. Both the cycling and impedance testing were controlled with CorrWare and Zplot softwares, while the collected data were fitted and analyzed with the corresponding softwares CorrView and ZView. Before each measurement all the test cells were left in Tenney Environmental Chambers for >3 h, where the temperature was controlled to be within ±0.1 °C.

In surface species analyses, anode half-cells were assembled using selected electrolytes of interest and cycled with similar protocols adopted in the EIS study. The MCMB anode was then retrieved, washed with DMC and diethylether repeatedly, and then dried at 40 °C under 10<sup>−2</sup> Torr vacuum overnight. Blank tests were conducted to confirm that the above rinsing protocol was effective in removing residual electrolyte solution trapped in anode while not damaging the surface layer.

All efforts in seeking for a nonaqueous, deuteriated NMR solvent that can effectively dissolve the interested alkylcarbonate salts have failed, due to the extremely low solubility of these SEI species in organic media.<sup>9</sup> In order to generate satisfactory NMR signal intensity from the surface species, the deuterolysis approach reported by Gireaud et al. was adopted instead,<sup>10</sup> and NMR spectra of the deuterolysis products were analyzed. Since the structural fingerprint of the interested semi-carbonate salts, i.e., their organic moieties, would remain in the form of deuteriated alcohols, the interpretation of the surface chemical analyses would not be affected. Thus, the surface species were collected by washing the dried MCMB anode with D<sub>2</sub>O at an approximate amount of 1 mL/cm<sup>2</sup>, and the concentrated D<sub>2</sub>O

solutions (~3.0 mL) were subjected to <sup>13</sup>C NMR analyses using either a 400 MHz Oxford or a 500 MHz Bruker spectrometer. In all cases tetramethylsilane (TMS) was used as internal or external reference. Due to the low concentrations of the surface species, prolonged data acquisitions were usually required to obtain a satisfactory signal-to-noise ratio (higher than 2), especially for the <sup>13</sup>C signals of the sp<sup>2</sup>-hybridized carbonyl functionalities.

## Results and Discussion

**1. Charge-Transfer Activation Energies and Its Dependence on Solvent Compositions.** State-of-the-art Li ion batteries employ nonaqueous electrolytes that are almost exclusively based on mixed solvents consisting of at least one cyclic carbonate such as EC and one or more linear carbonates such as DMC, EMC or DEC. The rationale behind the cyclic/linear combination proves more complicated than the simple considerations of bulk transport properties; instead, it involves an overall balance among the salt solubility, liquid range, solution viscosity, solvation sphere composition, and especially the electrochemistries with both oxidative and reductive electrode surfaces.<sup>11</sup> In Li ion chemistry, where the 4 V-class metal oxide cathodes coexist with the lithiated graphitic anodes of potentials close to metallic Li, the electrochemical stability is never realized through the thermodynamic inertness of the electrolyte components, but rather through the passivation of these strongly oxidative/reductive surfaces by the products generated during the initial decompositions of selected electrolyte components. So far, little is known regarding the exact interplay between the electrolyte compositions and the formation process of interface.<sup>11</sup> In the present studies, we selected the typical solvent mixtures of EC/DMC and EC/EMC as the model systems and attempted to establish such knowledge. Knowledge thus obtained should be universally applicable considering that the cyclic/linear combination is the skeletal formulation of almost all electrolytes in Li ion devices.

In the previous work, we carried out a series of electrochemical impedance analyses on graphite/electrolyte interfaces formed in two series of electrolytes (LiPF<sub>6</sub>/EC/DMC and LiBF<sub>4</sub>/EC/DMC at various EC/DMC ratios), and reported a unique correlation between the binary electrolyte composition and the activation energies derived from the temperature-dependences of the dominant impedance component, known as the charge-transfer process.<sup>8</sup> To further confirm that this correlation holds true not only for the electrolyte systems investigated therein but more likely for any cyclic/linear carbonate combination, we extended the EIS studies to a system considered more suitable for low temperature applications, which is LiPF<sub>6</sub>/EC/EMC with EC/EMC ratios at 10:90, 20:80, 30:70, 40:60, and 50:50, respectively. As an example, Figure 2a shows the Nyquist impedance plots collected at selected temperatures from the graphite/electrolyte interface formed in LiPF<sub>6</sub>/EC/EMC (30:70). Within the frequency range, two partially merged semicircles were almost always obtained, which enables a reliable deconvolution based on least-square approach using the equivalent circuit as described in the previous work.<sup>8</sup> By convention, these two semicircles were attributed to the Li<sup>+</sup> migration processes associated with “diffusion of naked Li<sup>+</sup> through SEI layer” at medium frequencies and “charge-transfer at lower frequencies”, though these nomenclatures might not necessarily reflect the nominal physical (for “SEI”) or chemical (for charge transfer) processes. At temperatures higher than ambient, a third semicircle, or the onset of it represented by a spike at 45 ° angle, might be observed for some samples at frequencies below 1 Hz, which corresponds to the diffusion of Li<sup>+</sup> in the graphene

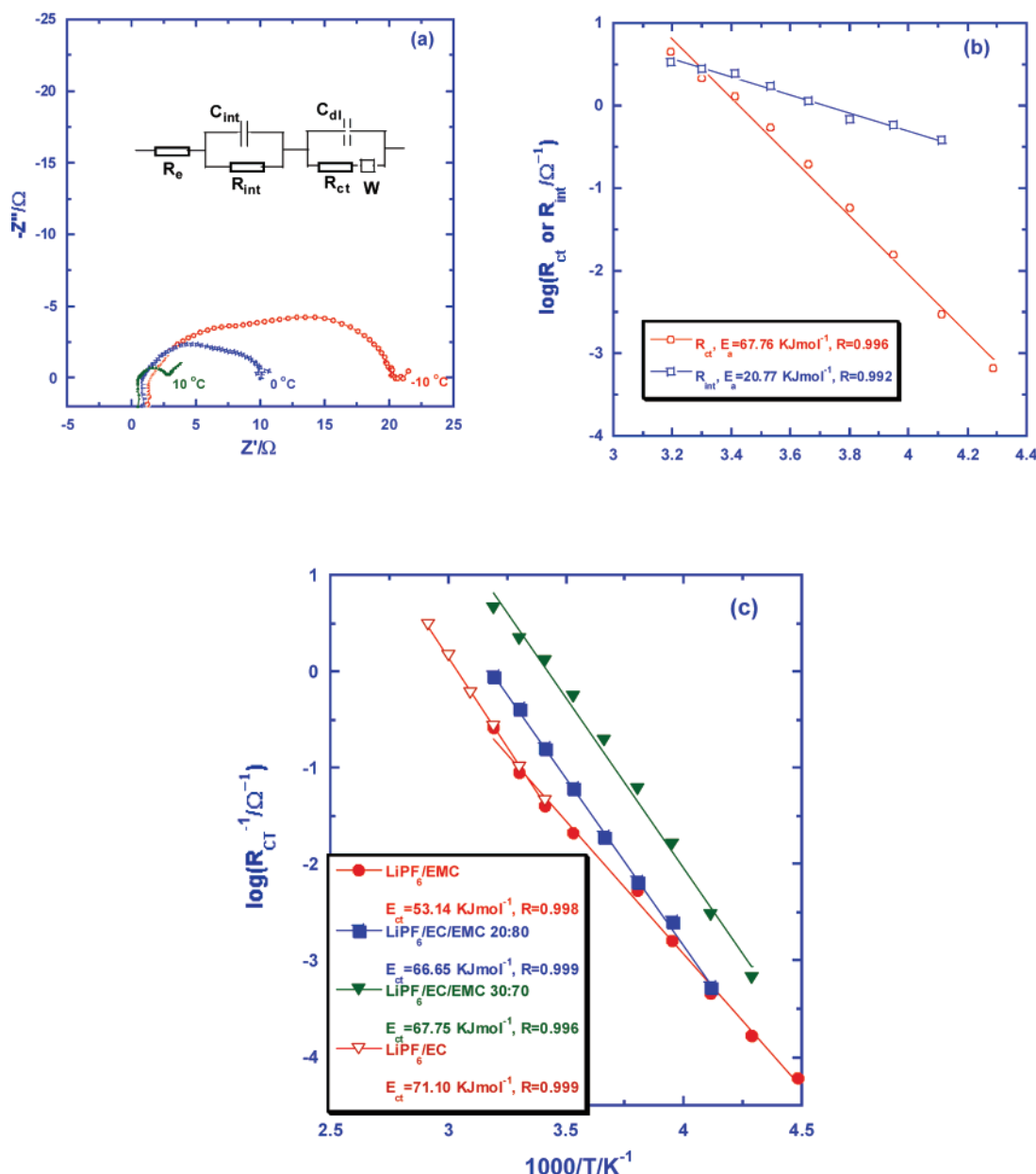


**Figure 2.** (a) The temperature-dependences of Nyquist plots of the graphite/electrolyte interphase formed in EC/EMC 30:70; (b) the comparison between the reciprocal interfacial ( $R_{int}$ ) and charge-transfer ( $R_{ct}$ ) components; and (c) Arrhenius behavior of the reciprocal resistances corresponding to charge-transfer components and the activation energies thus derived for the graphite/electrolyte interphases formed in LiPF<sub>6</sub>/EC/EMC at various carbonate ratios (only selected plots were shown for graphic clarity).

bulk that is usually described by a Warburg-type component. To maintain the graphic clarity, we chose not to display this component in Figure 2a. As has been discussed in our previous paper,<sup>8</sup> numerous authors have shown that the charge-transfer component is in fact closely associated with the chemistries of SEI, which will be further supported by the present work with evidence of chemical analysis.

Since all the AC impedance measurements were conducted at 0.15 V versus Li, which is the characteristic lithiation potential of graphitic structure, the corresponding reciprocal resistances to these two semicircles,  $1/R_{int}$  and  $1/R_{ct}$ , should be viewed as the measures of Li<sup>+</sup> transport through these two components SEI and charge transfer. Assuming that each transport step is a simple thermally activated process

$$\frac{1}{R_{(ct,int)}} = A_0 e^{-E_a/RT}$$

where  $A_0$ ,  $R$ , and  $E_a$  stand for a pre-exponential constant, the standard gas constant, and the activation energy, respectively, one can extract the activation energies for Li<sup>+</sup> transport during these processes from their Arrhenius behaviors by plotting  $\log(R^{-1})$  versus reciprocal temperature  $1/T$  plots:

$$E_a = -19.144 \times \text{slope (kJ} \cdot \text{mol}^{-1})$$

Excellent Arrhenius behaviors were demonstrated in Figure 2b for both  $R_{ct}$  and  $R_{int}$ , as indicated by the near unity values of the linearity indices ( $R$ ). The activation energies extracted from these transport processes for this particular interface (and for all other interfaces formed at different electrolyte compositions as well) fall into two rather distinct domains: 20–25 kJmol<sup>-1</sup> for the interfacial component and 50–70 kJmol<sup>-1</sup> for the charge-transfer component. According to the rationale of Abe and Ogumi et al., the former magnitude indicates a typical



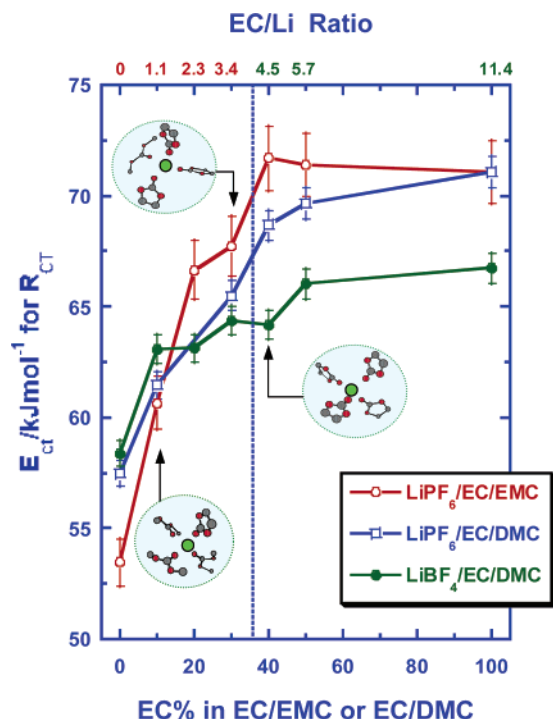


**Figure 3.** The correlation between the activation energies corresponding to the charge-transfer process and the ratio of cyclic to linear carbonate molecules in the bulk electrolyte solutions. The error margins in the figure were estimated from the linear fitting of the Arrhenius plots. Inset drawings: the variation of  $\text{Li}^+$  solvation sheath with EC availability in the solution.

intercalation process for naked  $\text{Li}^+$ , while the latter suggests an intercalation process of solvated  $\text{Li}^+$  that involves a much higher energy barrier associated with the breakup of its solvation sheath.<sup>12–14</sup> Since the charge-transfer component has been identified as the dominant contributor to cell impedance at low temperatures,<sup>8,11,15</sup> obviously due to its higher activation energy (or higher exponential index in its temperature-dependence), we would focus our interest on this component henceforward.

The EIS analyses were carried out systematically on the interfaces formed at all other EC/EMC ratios, along with two interfaces formed in electrolytes based on either neat EMC or neat EC to complete the entire composition range. The temperature dependences of reciprocal  $R_{\text{ct}}$  were plotted for a few selected interfaces in Figure 2c, and the activation energies for  $\text{Li}^+$  transport across the so-called charge-transfer component ( $E_{\text{ct}}$ ) were thus derived and shown in the legend. Consistently Arrhenius behaviors were exhibited by all interfaces investigated, with linear indices falling within 5% of unity. Immediately obvious from Figure 2c is that the interface in neat EMC exhibits the lowest  $E_{\text{ct}}$ , which increases as EC concentration in the electrolyte solutions.

To better view the correlation between electrolyte composition and  $E_{\text{ct}}$ , we plotted in Figure 3 the  $E_{\text{ct}}$  values derived for all these interfaces against the electrolyte compositions wherein they are formed, where EC/EMC ratio is also translated into a more enlightening EC/Li ratio in the upper horizontal axis. For comparison, the results for the interfaces formed in  $\text{LiPF}_6/\text{EC}/\text{DMC}$  and  $\text{LiBF}_4/\text{EC}/\text{DMC}$  series that have been reported in our previous paper are included.<sup>8</sup> As we expected, despite a wide spectrum of electrolytes studied, a rather universal correlation was obtained, which demonstrate such a “saturation” type of behavior that  $E_{\text{ct}}$  remains almost a constant whenever EC/Li is above 4, while dramatic decrease in  $E_{\text{ct}}$  occurs when EC/Li is below 3. In order to uncover the fundamental origins

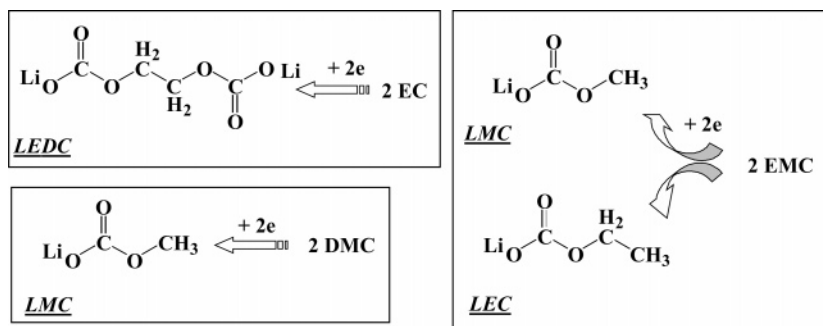
underneath this saturation phenomenon, we hereby are obliged to examine all possible contributing factors.

It has been generally agreed that, compared with other cyclic or linear carbonates, EC have higher reactivity toward the negatively charged graphitic surfaces, either due to the lower energy level of its intrinsic LUMO<sup>16</sup> or because of the  $\text{Li}^+$  coordination, which stabilizes the transition state of the single electron reduction of EC molecules in the supermolecular complexes.<sup>17</sup> In a solution based on mixed carbonate solvents, it is expected that the more electrophilic EC be preferentially adsorbed on graphite surface and consequently enjoys a precedence to linear carbonates DMC or EMC in being reduced upon the initial charging of the graphitic anode. If one assumes that an SEI originates from EC reduction corresponds to higher  $E_{\text{ct}}$  (which of course needs further experimental proof), a saturation behavior in  $E_{\text{ct}}$  vs EC% relation could ensue, because an SEI composed of EC origin exclusively would be formed when the EC population in the electrolyte solution is sufficiently high to adsorb on the active sites on the graphitic surface. In this scenario the threshold concentration of EC in Figure 3 should reflect the irreversible capacity associated with the formation of the interface, and it will also be dependent on the surface area of the graphitic anode. However, the fact that the threshold EC concentration is always located near 40% in all interface studied essentially rules out this possibility, because such a high threshold concentration cannot be accounted for by the rather small (10–15%) irreversible capacities as observed in the initial charging of the anode used in this study.<sup>8</sup> In addition, our experiments with anodes of different surface areas have also confirmed, with excellent reproducibility, that the activation energies under study ( $E_{\text{ct}}$ ) are independent of the electrode surface area but instead closely associated with the electrolyte bulk composition. Therefore, the rationale based on the preferred adsorption of EC and its higher reactivity on graphene surface cannot predict the correlation as seen in Figure 3.

On the other hand, the characteristic threshold concentration of EC, which corresponds to the well-accepted coordination number of  $\text{Li}^+$  in nonaqueous electrolytes (EC/Li ratio around 3–4) as determined by both theoretical and experimental approaches,<sup>17–20</sup> does strongly imply that  $\text{Li}^+$  solvation process should have been involved in shaping the correlation in Figure 3. If one reasonably assumes that EC molecule, which is distinctly more polar than the linear carbonates DMC and EMC, is preferentially coordinated by  $\text{Li}^+$  while conscripting its inner solvation sphere, then the saturation behavior that occurs at EC/Li  $\sim 4$  becomes immediately obvious: any electrolyte bulk composition with EC/Li above 4 would generate a homogeneous structure of  $\text{Li}^+$  solvation sheaths that is exclusively composed of EC molecules, while any electrolyte composition with EC/Li below 3 would suffer EC depletion, leading to the presence of linear carbonate in  $\text{Li}^+$  solvation sheaths. Considering the lower dielectric constants of those linear carbonates, it is logical to propose that the lower activation energies correspond to solvation sheaths containing them as members, whose disruption during the lithiation process constitutes lower energy barrier than do those sheaths that are saturated with EC molecules.

On the basis of the characteristic commonality for all the interfaces formed in various electrolyte systems, we concluded that the correlation in Figure 3 should actually reveal the transition of  $\text{Li}^+$  solvation sheath structure from EC/linear carbonate coexistence to EC dominance as EC population in bulk electrolyte increases. This dependence of solvation sheath composition on electrolyte bulk composition is the simultaneous

**SCHEME 2: Synthesized Reference Compounds LEDC, LMC, and LEC, Which Are Believed to Be the Reduction Products from EC, DMC, and EMC, Respectively, through the Single-Electron Path**



consequence of the  $\text{Li}^+$  preference in conscripting the cyclic EC as its solvation sheath members and the sufficiency/depletion of EC molecules in the bulk when EC concentration is above or below the critical threshold. Thus, an all-EC solvation sheath should be expected in solutions with EC content  $>30\%$  (equivalent to  $\text{EC/Li} \approx 3.5$ ), while linear carbonates DMC and EMC will inevitably appear in the sheath in solutions with EC content  $<20\%$  (or  $\text{EC/Li} < 2.3$ ).<sup>8</sup>

With the role of solvation identified in the correlation, we now turn to examine the role of SEI chemistry. While the initial attempt resorting to the “desolvation rationale”, as schematically described in Figure 1a,<sup>12–14</sup> has seemed to be able to predict the correlation as observed in Figure 3, we soon became aware of the fact that the above correlation is obtained under a post-SEI circumstance, i.e., for each electrolyte composition the charge-transfer impedance and its temperature dependence were extracted in the presence of an indigenous interface of specific chemical composition, which was originated from that particular electrolyte composition. Therefore, the SEI factor in the above correlation should not be overlooked; rather likely, if each SEI chemistry differs with the solvent composition, the effects of  $\text{Li}^+$  desolvation and  $\text{Li}^+$  diffusion through SEI layers would be too closely intertwined to be clearly distinguished by a phenomenological tool such as AC impedance technique.

On the other hand, there indeed is sufficient reason to believe that SEI chemistry should be closely related to the solvation sheath structure of  $\text{Li}^+$ . On the basis of the well-accepted “3D Model” proposed by Besenhard and Winter et al., the formation of the ternary graphite intercalation compounds (GIC) precedes the reductive breakdown of those solvent molecules in the sheath.<sup>21,22</sup> Therefore, if the cyclic carbonate molecules are preferentially conscripted by  $\text{Li}^+$  in the solvation sheath, they are also likely to be preferentially reduced during the initial charge of the graphitic anode by following the single-electron path as shown in Scheme 1a. In this picture, the probability of these solvent molecules in the sheath to participate in the surface reduction is amplified by their coordination with  $\text{Li}^+$ , which not only physically carries the solvent molecules to the reduction sites on graphene surface, as illustrated by Figure 1b, but also chemically catalyzes such reductions by activating certain bonds in the supermolecular complex  $\text{Li}^{+-(\text{solv})}_n$ .<sup>17,23</sup> As a result of such interplays, the source of the SEI ingredients could favor a particular solvent molecule, depending on both its probability to enter the  $\text{Li}^+$  solvation sheath and its sufficiency or depletion in the bulk solution, as suggested by the correlation between  $E_{\text{ct}}$  and the composition of the solvent mixture that we have observed for all the interfaces investigated.

It is rather interesting to note the difference between DMC and EMC systems as demonstrated in Figure 3. While  $E_{\text{ct}}$  for neat EMC solution is lower than that for neat DMC solution,

the introduction of EC in the former causes a more rapid increase, resulting in a crossover at  $\text{EC/Li}$  ratio  $\approx 1.0$ . This divergence in the “EC awareness” of DMC and EMC seems to arise from the difference between the coordination abilities of those two linear carbonates. In neat EMC or DMC solutions where no EC is available, the magnitudes of  $E_{\text{ct}}$  seems to be dictated by the easiness of desolvation, hence the relatively less polar EMC yields lower  $E_{\text{ct}}$  than DMC. In binary solvent mixtures, on the other hand, due to its higher dielectric constant, DMC tends to possess a higher opportunity of being recruited by  $\text{Li}^+$  in solvation sheath during its competition with EC. Thus, at a given EC concentration between 1.0 and 4.0, the average EC presence in solvation sheath is slightly lower for DMC- than for EMC-based systems, resulting in higher  $E_{\text{ct}}$  for the latter. We acknowledge that the gap in the  $E_{\text{ct}}$  values for those two electrolyte systems is not sufficiently large to ensure a reliable conclusion at this moment. Therefore, the above arguments should be subjected to further investigations, and caution should be taken in order not to over-interpret the results.

**2. Analyses of Surface Species and the Impact of  $\text{Li}^+$  Solvation Sheath Structure on SEI Chemistry.** The SEI formation model involving ternary GIC (Figure 1b)<sup>21</sup> and the variation of  $\text{Li}^+$  solvation sheath structure (Figure 3) jointly promoted us to infer that the SEI chemistries should vary with electrolyte composition, and that very likely the chemistry composition of interface is not colinear with that of the bulk electrolyte composition. In other words, the contribution from cyclic and linear carbonates to SEI formation is not in simple proportion to their respective populations in the bulk electrolyte solutions, as indicated by the characteristic curves in Figure 3. For example, the interfaces formed in electrolytes with  $\text{EC/Li}$  ratios  $<2.3$  ( $\text{EC}\% < 20$ ) and  $>3.5$  ( $\text{EC}\% > 30$ ) should vary distinctly, with the former possessing reduction products from linear carbonates while the latter dominated by EC reduction products, although in both electrolytes the linear carbonates are the majority cosolvent. This asymmetry is undoubtedly introduced by  $\text{Li}^+$  preference in forming its solvation sheath, which serves as an enrichment core of EC for the surface reductions. To confirm the above hypothesis, we performed a series of direct chemical analyses on the interfaces formed in selected electrolytes by using solution NMR techniques, which is apt to distinguish the minute structural differences of alkyl or alkene moieties that are likely originated from cyclic and linear carbonates. An additional advantage for NMR technique is that it can selectively characterize surface species of interest only, such as the alkylcarbonates that are essential for the SEI function, while overlooking most of the inorganic impurities deposited on the electrode surface that would usually complicate the surface analyses.

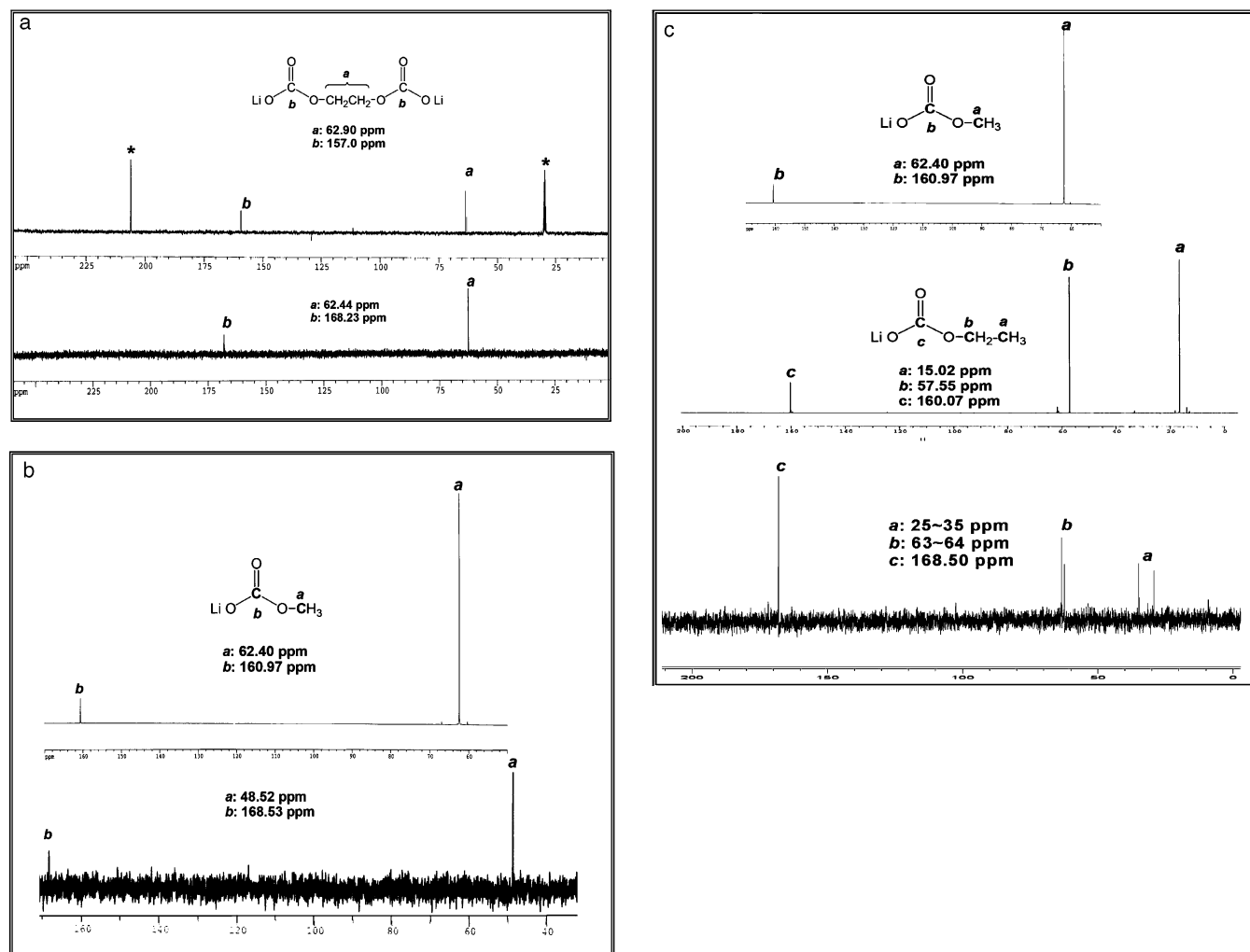


**Figure 4.** (a) Comparison between the <sup>13</sup>C NMR spectra of authentic lithium ethylene dicarbonate (upper) and the surface species collected from the graphitic anodes cycled in LiPF<sub>6</sub>/EC (below). The asterisks mark the solvent signals. (b) Comparison between the <sup>13</sup>C NMR spectra of authentic lithium methylcarbonate (upper) and the surface species collected from the graphitic anodes cycled in LiPF<sub>6</sub>/DMC (below). (c) Comparison between the <sup>13</sup>C NMR spectra of authentic lithium methylcarbonate (upper), lithium ethylcarbonate (middle) and the surface species collected from the graphitic anodes cycled in LiPF<sub>6</sub>/EMC (below).

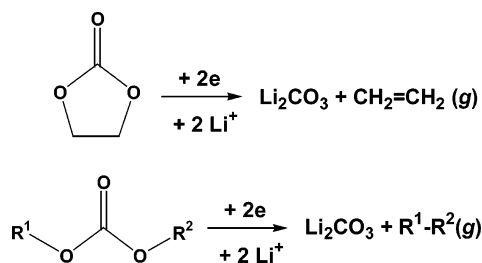
Previously, as part of our attempt to identify the basic chemical building blocks of SEI, we have synthesized a homologous series of semi-carbonates as the model lithium alkylcarbonates that were believed to be the major reduction products from the commonly used cyclic and linear carbonates through the single-electron paths as described in Scheme 1.<sup>6,7,9</sup> Part of those reference compounds include lithium methylcarbonate (LMC), lithium ethylcarbonate (LEC), and lithium ethylenedicarbonate (LEDC), corresponding to the reductions of DMC, EMC, and EC, respectively, as summarized in Scheme 2.

The structural knowledge accumulated on these building blocks, especially their FTIR and NMR spectra, provides a reliable basis for the accurate identification of the actual surface species collected from the electrodes in Li ion devices. Already we have benefited from the availability of these authentic semi-carbonates in interpreting the surface spectra data,<sup>6,7</sup> while modeling efforts based on their bulk physicochemical properties are also underway. In the present work, we also relied on the NMR spectra of these standard references for the accurate recognition of surface species collected from the interfaces of interest. Figure 4a–c summarized the efforts to establish a baseline of comparison, in which the <sup>13</sup>C NMR spectra of the surface species that were formed in the three electrolytes using

neat solvent (LiPF<sub>6</sub>/EC, LiPF<sub>6</sub>/DMC, and LiPF<sub>6</sub>/EMC) were listed against those of the corresponding reference compounds LEDC, LMC, and LEC. Despite the fact that the <sup>13</sup>C NMR spectra for all surface species were collected from their deuterolyzed products, their characteristic structural information was faithfully maintained in the corresponding deuteriated alcohols which contain the alkyl skeleton of the original lithium alkylcarbonates. Obviously there is a general agreement between the spectra of the synthesized authentic alkylcarbonates and the corresponding deuterolyzed products of the surface species, in terms of both the number of carbon nuclei detected and their chemical shifts, which have been labeled in the figures to indicate the assignment. The common feature of those spectra is the co-presence of carbonyl and alkyl/alkoxy functionalities at ~160 and ~60 ppm, which firmly excludes the possibility of a two-electron alternative reduction path of those alkene or dialkylcarbonates, because by this mechanism the alkyl/alkoxy moieties would be lost in the form of alkene or alkane, instead of becoming part of the SEI (Scheme 3).

The above two-electron path was first proposed for carbonate reduction on graphite surface,<sup>24</sup> and was later displaced by Aurbach's single-electron path based on their systematic work on graphite surface chemistry.<sup>3</sup> Since no NMR spectra have ever been collected on surface species formed on graphitic anodes,



**SCHEME 3: Two-Electron Reduction Path for Cyclic and Linear Carbonates<sup>a</sup>**

<sup>a</sup> Note that alkyl/alkoxy moieties would be absent in SEI.

Figures 4a–c can be regarded as the first of the kind, which reconfirmed the single-electron path of Scheme 1, and provided additional support to the arguments that the prevalent existence of  $\text{Li}_2\text{CO}_3$  in SEI were actually generated by further reduction of semi-carbonate or effect of ambient moisture rather than direct reduction of alkene or dialkyl carbonates.<sup>25</sup>

The only complication in the baseline comparison is the spectrum of the surface species formed in  $\text{LiPF}_6/\text{EMC}$  (Figure 4c), which showed an extra pair of alkyl signals for ethoxy substructure ( $-\text{O}-\text{CH}_2-\text{CH}_3$ ). Note that the reduction of EMC would produce both LMC and LEC simultaneously, therefore the extra carbon nuclei at 63–64 ppm should reflect the competitive reductions leading to ethoxy- and methoxy-containing moieties, which are presumably LEC and LMC, respectively. The extra signal at 25–35 ppm, on the other hand, could arise from lithium ethoxide instead of LEC, but  $^7\text{Li}$  NMR data has not been able to support this possibility. In general it seems that the main SEI components generated in those three neat solvent electrolytes are indeed the corresponding semi-carbonate salts that were formed from the single-electron reduction path as suggested by Scheme 1. At least in the above cases the conclusions drawn by Aurbach et al.<sup>3</sup> and Ein-Eli<sup>4</sup> on the chemical nature of SEI hold true (Scheme 4).

The above simple picture of the interface chemistry came as a surprise, as one would anticipate a more complicated scenario considering the collection of possible parallel or consequential reduction paths in competition, generating monomeric as well as oligomeric etheric species besides alkoxides and alkylcarbonates. This simplicity could be partially attributed to the selective extraction by the NMR solvent, which probably prefers to dissolve the salts rather than non-ionic species, such as polymeric or oligomeric ethers. According to the  $^7\text{Li}$ ,  $^{19}\text{F}$ , and  $^{31}\text{P}$  NMR spectra collected simultaneously (not shown), the only ionic lithium species detected in the solutions are  $\text{LiF}$ ,  $\text{LiOD}$ , which is the deuterolyzed form of all the lithium salts, and  $\text{LiPF}_6$ , which remained/trapped on the anode surface (The identification of the intact  $\text{LiPF}_6$  is unmistakable, although surprising, due to the unique heptet split pattern of  $^{31}\text{P}$  by its neighboring  $^{19}\text{F}$  nuclei).

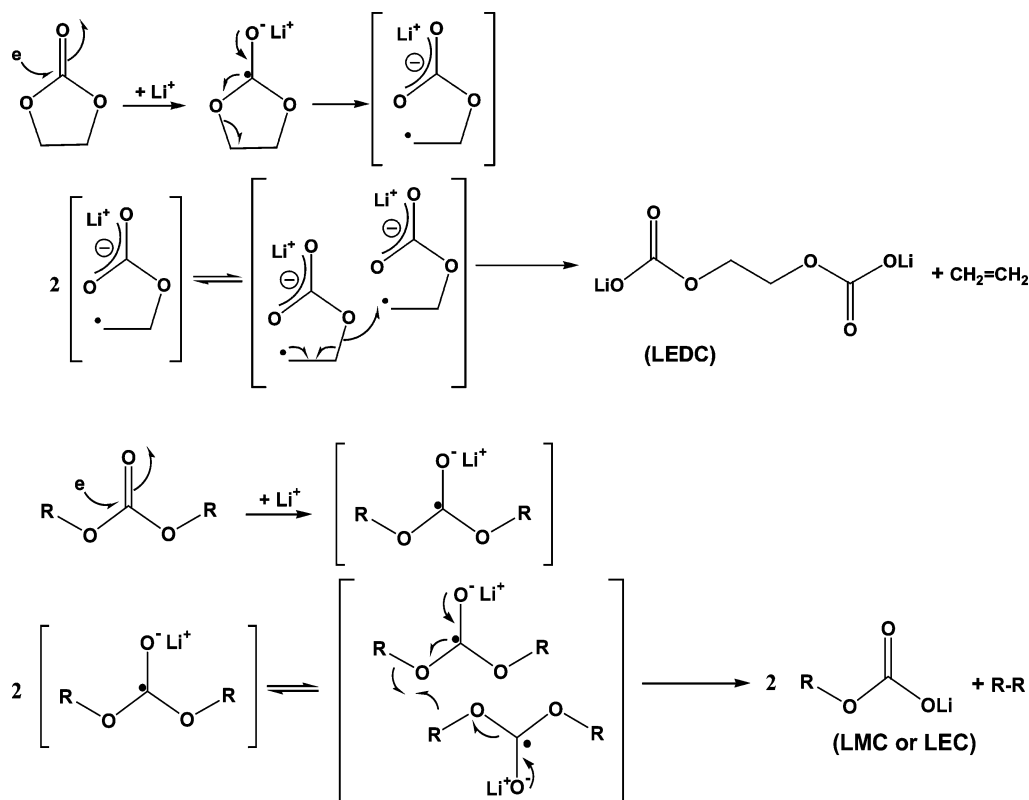
More complicated pictures of surface chemistry were obtained when binary instead of neat solvents were used in the electrolytes. Figures 5 and 6 summarized the  $^{13}\text{C}$  NMR spectra of the deuterolyzed surface species which were collected from interfaces formed in two series of electrolytes:  $\text{LiPF}_6$  in EC/DMC and  $\text{LiPF}_6$  in EC/EMC. Though still composed of two groups of peaks corresponding to carbonyl ( $\sim 160$  ppm) and alkyl ( $\sim 30$  ppm) or alkoxy moieties ( $\sim 60$  ppm), a variety of functionalities that share the carbonate-origins were now detectable. For example, the spectra in Figure 5 demonstrated a collection of signals between 60–70 ppm corresponding to at least six kinds of  $^{13}\text{C}$  nuclei, which should all share the alkoxy substructure of either  $[-\text{O}-\text{CH}_2\text{CH}_2-\text{O}-]$  or  $[-\text{O}-\text{CH}_3]$ . While it is impos-

sible to accurately assign each signal, we believe that they should arise from the alkoxy sub-structures in semicarboxylate salts and oligomeric ethers (as represented by the structures of the original SEI species before deuterolysis in Figure 5). The latter are the further reduction products of semi-carbonates from either EC or DMC. A similar effort at assignment was also made for the spectra shown in Figure 6. The  $^{19}\text{F}$  and  $^{31}\text{P}$  NMR collected simultaneously on some of these graphite surfaces showed an enrichment of new Li-containing species in addition to  $\text{LiOD}$ ,  $\text{LiF}$ ,  $\text{LiPO}_x\text{F}_y$ , and the intact  $\text{LiPF}_6$  that were observed in the cases of neat solvent-based electrolytes. However, a more detailed assignment was not possible due to the broad and the overlapping multiplets.

On the other hand, while the  $^{13}\text{C}$  spectra shown in either Figures 5 or 6 cannot rule out the possible formation of oxalates,<sup>5</sup> the absence of  $^{13}\text{C}$  nuclei at 20–30 ppm in Figure 5 did exclude the presence of any carboxylate  $[-\text{CH}_2\text{C}(\text{O})\text{OLi}]$  or alkene  $[-\text{CH}_2-\text{CH}_2\text{CH}_2-]$  substructures on the surface, hence overthrowing the theoretical prediction based on ab initio computations that the thermodynamically favored lithium butylene dicarbonate  $[\text{CH}_2\text{CH}_2\text{OC}(\text{O})\text{OLi}]_2$  or other carboxylates be the main components of SEI.<sup>17,23</sup> In view of the higher sensitivity of NMR in distinguishing subtle variations in the locality of  $^{13}\text{C}$  nuclei as compared with other spectroscopic techniques, we are confident about the above exclusion of higher order semi-carbonates and carboxylates from the candidate SEI components.

More interesting to us, there indeed appears to be a firm dependence of the surface chemistry on electrolyte composition in both binary electrolyte systems, which are  $\text{LiPF}_6$  in EC/DMC at 10:90 and 50:50, and  $\text{LiPF}_6$  in EC/EMC at 10:90, 20:80, and 30:70, respectively. In the former system, since the signals generated by the EC- and DMC-originated species, i.e.,  $[-\text{O}-\text{CH}_2\text{CH}_2-\text{O}-]$  or  $[-\text{O}-\text{CH}_3]$ , would fall in the close vicinity of 60–70 ppm and are essentially undistinguishable, it would be difficult to tell whether the extent of DMC-reduction increases as EC/DMC ratio changes from 50:50 to 20:80. However, we can still establish the correlation based on the following two facts: (1) the relatively simple spectrum of the surface chemistry formed in EC/DMC 50:50 (Figure 5, upper) bears close resemblance to that formed in the neat solvent-based electrolytes (Figures 4a); and (2) the much diversified signal collection in EC/DMC 10:90 (Figure 5, below) suggests that new species appear as the result of the extensive DMC participation in SEI chemistry. In other words, with EC/DMC ratio at 50:50 (or EC/Li ratio  $\approx 5.7$ ), the surface species seemed to predominantly consist of the EC-originated product LEDC, while with EC/DMC ratio at 10:90 (or EC/Li ratio  $\approx 1.1$ ), the reduction of DMC is inevitable because of its presence in the  $\text{Li}^+$  solvation sheath now. In the latter case the SEI should consist of the mixture of LEDC and LMC, along with other etheric and alkoxide species.

More unambiguous evidence comes from the EMC-containing system. Because the  $^{13}\text{C}$  signals of the methyl moiety  $[-\text{CH}_2-\text{CH}_3]$  locate at 20–30 ppm, which are well separated from any signals of EC-originated products, they serve as a reliable indicator for the EMC reduction. Thus, the spectra in Figure 6, which corresponds to the interfaces formed in three electrolytes with varying EC/EMC ratios, paints a dynamic picture of how EMC-participation in the surface chemistry changes with electrolyte composition. At EC/EMC of 30:70 (or EC/Li  $\approx 3.4$ ), although EMC is the dominant species in bulk, the surface species are almost exclusively from the reduction products of EC, among which LEDC appear to be the leading component

SCHEME 4: Proposed Mechanism of the Single-Electron Reductions of Cyclic and Linear Carbonates<sup>a</sup>

<sup>a</sup> Note that in this path 50% of the alkyl/alkoxy moieties would be converted in the form of semicarbonate salts and remain in SEI, while the other 50% is lost.

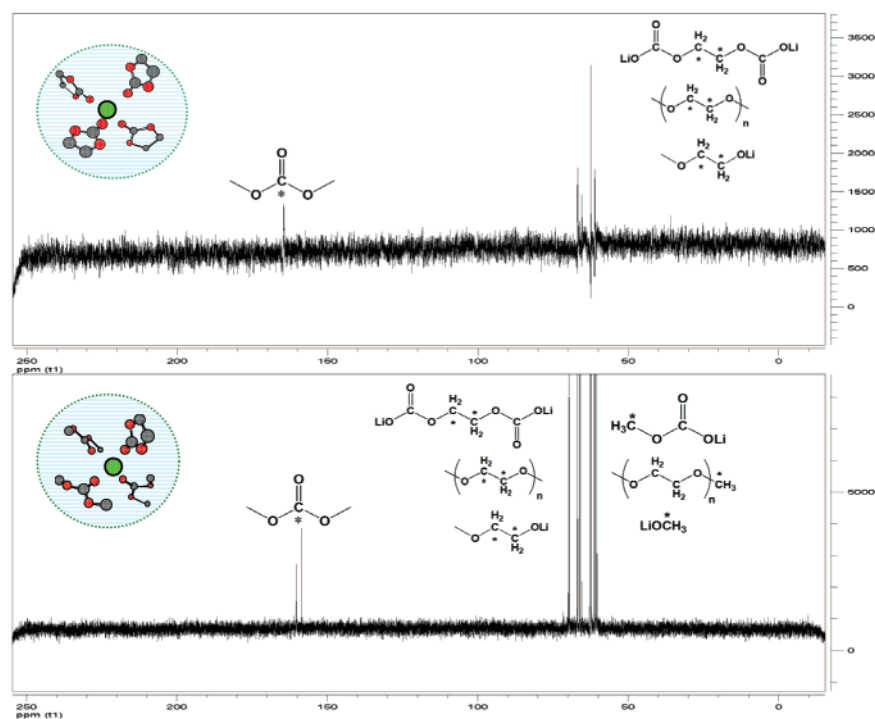


**Figure 5.** <sup>13</sup>C NMR of surface species collected from graphitic anodes cycled in LiPF<sub>6</sub>/EC/DMC 50:50 (upper) and 10:90 (below). Inset drawings: the Li<sup>+</sup> solvation sheath composition and the structure of the original SEI species. The asterisks mark the probable <sup>13</sup>C nuclei that generate the signals.

based on the comparison with baseline in Figure 4a. If we accept the coordination number of Li<sup>+</sup> in carbonate-based solutions as 4 based on previous theoretic and experimental works,<sup>17–20</sup> then statistically there should be at least one EMC molecule in each of the Li<sup>+</sup> solvation sheath in this electrolyte, in addition

to the overwhelming EMC population in the solution. Nevertheless, the EMC-originated species are hardly detectable in the interface formed in this solution, which could be the result of the higher reactivity of EC in the solvation sheath. This asymmetry corroborates our argument that the cyclic carbonates,

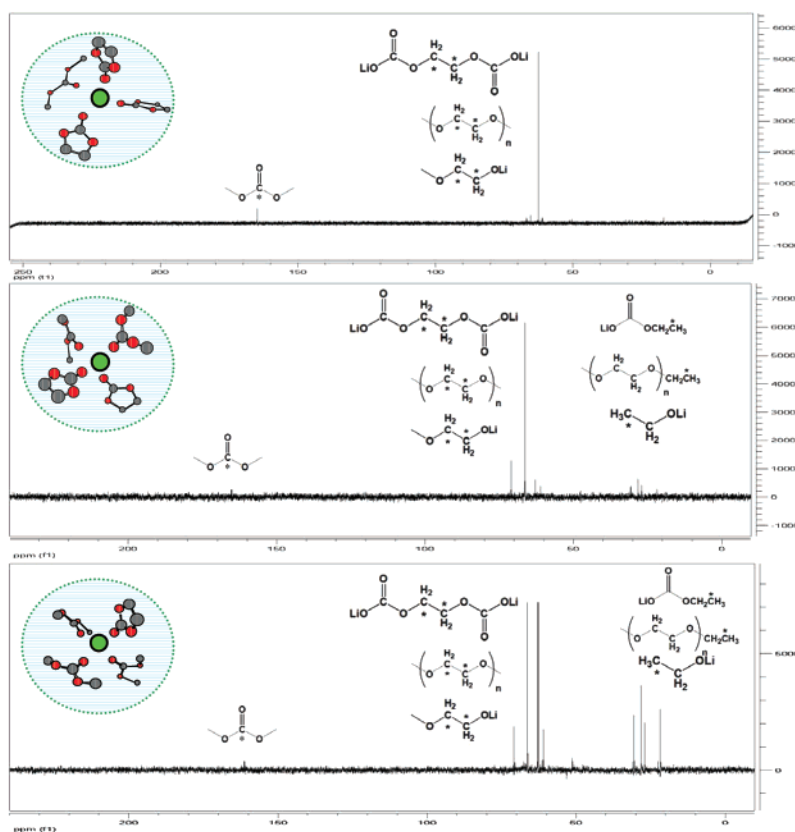


**Figure 6.**  $^{13}\text{C}$  NMR of surface species collected from graphitic anodes cycled in  $\text{LiPF}_6/\text{EC}/\text{EMC}$  30:70 (upper), (b) 20:80 (middle), and (c) 10:90 (below). Inset drawings: the  $\text{Li}^+$  solvation sheath composition and the structure of the original SEI species. The asterisks mark the probable  $^{13}\text{C}$  nuclei that generate the signals.

which are preferentially conscripted by  $\text{Li}^+$  in solvation sheath, will also be preferentially reduced during the formation of SEI, and echoes with the in situ FTIR work carried by Zhuang et al. on a nonporous electrode for a similar electrolyte system.<sup>6</sup>

The signals for the EMC-reduction products start to appear around 20–30 ppm at EC/EMC of 20:80 ( $\text{EC}/\text{Li} \approx 2.3$ , or averagely two EMC molecules in each solvation sheath), represented by a variety of methyl-containing products as indicated in Figure 6 (middle). The surface chemistry therefrom should consist of the mixture of both EC- and EMC-originated species, with LEDC still as the major ingredient. The abundances of these EMC-originated species further intensify at EC/EMC of 10:90 ( $\text{EC}/\text{Li} \approx 1.1$ ), because by then EMC has become the majority in the  $\text{Li}^+$  solvation sheath (statistically three EMC molecules in each sheath). The surface chemistry, consequently, is characteristic of EMC-reduction as indicated by the resemblance of its  $^{13}\text{C}$  NMR spectrum to Figure 4c, even though EC-originated species are still present because of its precedence to be recruited by  $\text{Li}^+$  into the solvation sheath and its higher tendency to be reduced. From Figure 3 we know that such interfaces of high linear carbonate source would correspond to a lower kinetic energy barrier to  $\text{Li}^+$  transport at subambient temperatures as compared with the interfaces expected from the popular electrolyte formulations, where EC content is usually higher than 20%. However, such a “pervious” interface would not provide effective protection to the graphene structure against persistent solvent co-intercalation and reduction as an EC-originated SEI would do, while its stability at elevated temperatures also prove to be problematic.<sup>11</sup> The electrolytes used in commercial Li ion devices are the results of compromises among the above considerations.

The transition process of surface chemistry as observed in Figures 5 and 6 corresponds well with the correlation observed

in Figure 3. On the basis of these convincing evidence from NMR analyses, we believe that our hypotheses on the interplay among electrolyte composition,  $\text{Li}^+$  solvation sheath structure and its role in surface chemistry, especially as a result the asymmetric contribution from cyclic and linear carbonate to interface chemistry, have been confirmed. Apparently, despite its relatively low population in the bulk solutions, EC participation in SEI chemistry has been asymmetrically amplified due to both its higher affinity to  $\text{Li}^+$  and its higher reactivity toward surface reduction. This precedence of EC in surface chemistry, in combination with its nearly “omnipresence” in all electrolyte formulations currently used in commercial Li ion devices, makes this cyclic carbonate solvent the central component in defining key performances of this battery chemistry. The chemical origin of the SEI, i.e., whether exclusively EC-originated or with presence of linear carbonate-originated, would eventually determine the performance of the Li ion devices, especially at sub-zero temperatures.

It should be emphasized that the above conclusion, although extracted from interfaces formed in EC/DMC and EC/EMC systems, should be applicable in principle to all electrolyte systems that are based on cosolvents of high dielectric constant and cosolvents of low viscosity. The formulation of an electrolyte solution that can simultaneously offer both stability at elevated temperatures and facile kinetics at subzero temperatures requires better understanding about how these cosolvents interact with  $\text{Li}^+$  and participate in the formation of the most important subcomponent in the Li ion device.

## Conclusions

While in previous work it has been shown that it is possible to reveal the structure of  $\text{Li}^+$  solvation sheath in

nonaqueous electrolytes from impedance analyses, the present work sheds further light on the interplay between electrolyte bulk composition and Li<sup>+</sup> solvation sheath structure and how they determine the graphite/electrolyte interface chemistry. Due to the selectivity of Li<sup>+</sup> in recruiting EC as its solvation sheath member, the participation of EC in formation chemistry of SEI is asymmetrically amplified as compared with other linear carbonate cosolvents. The correlation between charge-transfer activation energies and bulk electrolyte composition predicts that various interface chemistries with cyclic or linear carbonate sources would exhibit distinct tolerances toward Li<sup>+</sup> transport, especially at sub-zero temperatures. The fundamental understanding about how cyclic and linear carbonate share the responsibility of forming SEI will serve as a useful guideline to manipulate the SEI chemistry for the purpose of improving the performance of Li ion devices at low temperatures.

**Acknowledgment.** This work was partially funded by Office of FreedomCar and Vehicle Technologies of US Department of Energy, under contract number DE-AI01-99EE5061. The technical assistance from Dr. Yinde Wang (UMD) with NMR experiments is highly appreciated. One of the authors (TBC) is grateful to the summer internship program sponsored by Cadet Command of the U.S. Army.

## References and Notes

- (1) Fong, R.; von Sacken, U.; Dahn, J. R. *J. Electrochem. Soc.* **1990**, *137*, 2009.
- (2) Peled, E. *J. Electrochem. Soc.* **1979**, *126*, 2047.
- (3) Aurbach, D.; Ein-Eli, Y.; Markovsky, B.; Zaban, A.; Lusk, S.; Carmeli, Y.; Yamin, H. *J. Electrochem. Soc.*, **1995**, *142*, 2882.
- (4) Ein-Eli, Y. *Electrochem. Solid-State Lett.* **1999**, *2*, 212.
- (5) Zhuang, G.; Ross, P. *Electrochem. Solid State Lett.*, **2003**, *6*, A136.
- (6) Zhuang, G. V.; Xu, K.; Yang, H.; Jow, T. R.; Ross, P. N.; Jr. *J. Phys. Chem. B* **2005**, *109*, 17567.
- (7) Zhuang, G. V.; Yang, H.; Ross, P. N., Jr.; Xu, K.; Jow, T. R. *Electrochem. Solid-State Lett.*, **2006**, *9*, A64.
- (8) Xu, K. *J. Electrochem. Soc.* **2007**, *154*, A162.
- (9) Xu, K.; Zhuang, G. V.; Allen, J. L.; Lee, U.; Zhang, S.; Ross, P. N.; Jr.; Jow, T. R. *J. Phys. Chem. B* **2006**, *110*, 7708.
- (10) Gireaud, L.; Grugeon, S.; Laruelle, S.; Pillard, S.; Tarascon, J. -M. *J. Electrochem. Soc.* **2005**, *152*, A850.
- (11) Xu, K. *Chem. Rev.* **2004**, *104*, 4303.
- (12) Abe, T.; Fukuda, H.; Iriyama, Y.; Ogumi, Z. *J. Electrochem. Soc.* **2004**, *151*, A1120.
- (13) Abe, T.; Ohtsuka, M.; Sagane, F.; Iriyama, Y.; Ogumi, Z. *J. Electrochem. Soc.*, **2004**, *151*, A1950.
- (14) Abe, T.; Sagane, F.; Ohtsuka, M.; Iriyama, Y.; Ogumi, Z. *J. Electrochem. Soc.* **2004**, *152*, A2151.
- (15) Zhang, S.; Xu, K.; Jow, T. R. *J. Power Sources* **2003**, *115*, 137.
- (16) Chung, G.; Kim, H.; Yu, S.; Jun, S.; Choi, J.; Kim, M. *J. Electrochem. Soc.* **2000**, *147*, 4391.
- (17) Wang, Y.; Nakamura, S.; Ue, M.; Balbuena, P. B. *J. Am. Chem. Soc.* **2001**, *123*, 11708.
- (18) Blint, R. J. *J. Electrochem. Soc.* **1995**, *142*, 696.
- (19) Fukushima, T.; Matsuda, Y.; Hashimoto, H.; Arakawa, R. *Electrochem. Solid-State Lett.* **2001**, *4*, A127.
- (20) Matsuda, Y.; Fukushima, T.; Hashimoto, H.; Arakawa, R. *J. Electrochem. Soc.* **2002**, *149*, A1045.
- (21) Besenhard, J. O.; Winter, M.; Yang, J.; Biberacher, W. *J. Power Sources* **1993**, *54*, 228.
- (22) Wagner, M. R.; Albering, J. H.; Moeller, K. -C.; Besenhard, J. O.; Winter, M. *Electrochem. Commun.*, **2005**, *7*, 947.
- (23) Wang, Y.; Nakamura, S.; Tasaki, K.; Balbuena, P. B. *J. Am. Chem. Soc.* **2002**, *124*, 4408.
- (24) Dey, A. N.; Sullivan, B. P. *J. Electrochem. Soc.* **1970**, *117*, 222.
- (25) Inaba, M.; Ogumi, Z. In *Li Ion Batteries: Solid Electrolyte Interphase*; Balbuena, P. B., Wang, Y., Eds.; Imperial College Press: Singapore, 2004; Chapter 4.